SEMaTA (Sustainable Energy and Material at Tropical Area)
Journal homepage: https://talenta.usu.ac.id/semata

Virtual manufacturing and experimental validation of distortion in laser welding of butt joint

Anggara Joemora Pardi Bakara*[1]
[1]Hochschule Aalen, Aalen, 73430, Germany
*Corresponding Author: joemorapardi362@gmail.com

ARTICLE INFO

Article history:
Received : March 15th, 2026
Revised: April 20th, 2026
Accepted: April 30th , 2026
Available online: September 11th, 2026

E-ISSN:
P-ISSN:

How to cite:
Anggara Joemora Pardi Bakara,"Virtual manufacturing and experimental validation of distortion in laser welding of butt joint ", Junal SEMaTA (Sustainable Energy and Material at Tropical Area) Vol. 01, No. 02 , pp.11-21, September 2026.

ABSTRACT

This research explores the distortion behavior of welded butt joints using virtual manufacturing (VM) analysis. The main aim is to compare and validate the simulation outcomes generated through APDL (Ansys Parametric Design Language) with experimental results. A nonlinear, three-dimensional finite element method (FEM)-based VM framework is utilized for the simulations. To enhance modeling efficiency, the complexity of the weld geometry and the impact of transient temperature distribution are deliberately reduced. The heat input for the butt joint is simulated using Goldak's double ellipsoid model. Furthermore, a flow curve corresponding to S235 low-carbon steel is applied, incorporating a constant strain rate of 0.001 s^{-1}, modeled using a nonlinear isotropic plasticity approach and the von Mises yield criterion. The results demonstrate that simplifying the weld geometry and material definitions substantially reduces the pre-processing time without significantly compromising the accuracy of distortion predictions. Both simulation methods exhibited high precision in forecasting angular distortion, with an average deviation of approximately 20%, indicating no significant practical discrepancy. Therefore, the simplified modeling strategy, omitting detailed heat source modeling, temperature calibration, and complex material characterization, is recommended for scenarios where time constraints exist and a moderate level of accuracy is sufficient.

Keyword: Virtual manufacturing, APDL, Experimental validation, Goldak's double ellipsoid method, Angular distortion.

1. Introduction

The integration of Virtual Manufacturing (VM) processes into contemporary engineering is crucial for addressing challenges related to the increasing demand for both the quality and quantity of manufactured goods. Finite Element Method (FEM)-based VM constitutes a core component of Virtual Engineering, enabling the digital representation of real-world manufacturing processes through numerical modeling. Fundamentally, the primary aim of VM is to replicate the entire manufacturing process in a virtual environment to enhance decision-making and ensure effective quality control throughout production [1]-[2]. Many VM engineers utilize three-dimensional models to develop simulations that closely replicate actual manufacturing operations [3]. The essential principle underlying the fusion welding process involves heating two or more materials, either similar or dissimilar, until they reach their melting points, followed by joining them together as they begin to cool. Among various fusion welding techniques, laser welding is widely adopted due to its adaptability, high efficiency and suitability for a broad spectrum of plate thicknesses in engineering applications [4]-[5]. One prevalent joint configuration is the butt joint, which is extensively used in welding pipes and tubes positioned at perpendicular angles. Typically, butt joint welding necessitates multiple welding passes, particularly when working with thicker pipes or tubes [6].

In modern engineering practices, welding technology is extensively employed in the fabrication of lightweight structures composed of thin plates. Nonetheless, distortions that occur during the welding process are often challenging to rectify and may result in defects that adversely affect the integrity and design of the final product

[7]. Such distortions compromise dimensional precision, leading to misaligned structural elements, poor joint conformity and diminished visual appeal. Although welding remains a widely used manufacturing technique, the presence of distortion can significantly undermine the final product quality and escalate production costs, particularly in terms of maintenance [8]. Welding-induced distortions primarily result from thermally generated stresses that are unevenly distributed in joints lacking proper restraint. The three most common forms of distortion observed in welding processes include longitudinal shrinkage (along the weld line), transverse shrinkage (across the weld line), and angular distortion (rotational deformation about the weld line). Several factors, such as joint configuration, heat input parameters, and the sequence of welding operations, play critical roles in determining the magnitude of distortion [9]. Performing repair welding not only introduces project delays but also adds to overall expenses. Therefore, by accurately predicting the extent of welding distortion, engineers can reduce the need for corrective work through the application of reverse design methodologies and appropriate distortion allowances [10].

Accurately predicting welding distortion is critical for mitigating its adverse effects on manufacturing outcomes. The primary approaches for distortion prediction are generally classified into experimental, analytical, and numerical methods [11]. Among these, computer-aided numerical techniques, such as the Finite Element Method (FEM), serve as powerful tools for analyzing potential deformations by simulating welding-induced distortion patterns using real-world manufacturing parameters [12]. Since their development, numerical simulations have become an integral part of the welding process, enabling the anticipation of experimental outcomes prior to actual welding. The application of three-dimensional models plays a vital role in enhancing the precision of predictions related to post-weld deformation and stress distribution within welded joints.

One of the primary functions of the Finite Element Method (FEM) in welding applications is to predict the extent of distortion that may occur during the welding process through numerical analysis. FEM acts as a preventive measure prior to actual welding, enabling engineers to minimize the risk of undesirable deformations [13]. In welding simulations, Finite Element Analysis (FEA) typically involves two main components: thermal analysis and mechanical analysis [14]. Thermal computations are carried out at each phase of heating and cooling to support accurate analysis [15]. Nevertheless, certain computational limitations pose challenges in achieving predictions that perfectly match real-world outcomes. Despite these constraints, advancements in simulation software and numerical methodologies have significantly enhanced the understanding of welding processes, allowing for reasonably accurate predictions of thermal cycles and welding-induced distortions [16].

Researchers in the field of Finite Element Method (FEM) have consistently sought to reduce the computational time and complexity associated with transient linear problems through the use of numerical simulations [17]. Mato and Zdenko conducted an analysis of a butt joint weld to investigate the residual stresses and distortions induced by the welding process [18]. Their findings indicated that the use of a three-dimensional solid numerical model had minimal influence on the resulting temperature distribution. Accurately predicting angular distortion is particularly important for effectively mitigating its adverse effects.

Over the past few decades, significant research has been dedicated to the development of heat source models tailored to various welding techniques. Examples include the Gaussian or elliptical heat source model for Tungsten Inert Gas (TIG) welding at low current levels, the double-ellipsoidal heat source model for Metal Inert Gas (MIG) welding and the combined double-ellipsoidal and EHGC (Exponentially-Tapered Peak Value of Heat Flux in a Gaussian Cylinder) model for plasma arc welding [19]. In the late 1960s, Pavalec introduced a circular disc heat source model characterized by a Gaussian distribution applied to the surface of the workpiece. Subsequently, Goldak advanced the field by developing the double-ellipsoidal heat source model specifically for finite element (FE)-based welding simulations. Goldak's Double Ellipsoid model is illustrated in Figure 1 [20].

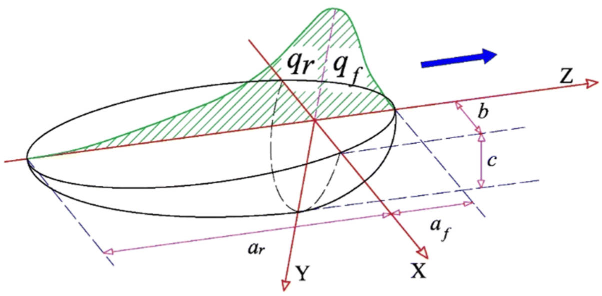

Figure 1. Goldak's double ellipsoid heat source model

The power density of the heat flux in the front section (Q_{vf}) of the heat source can be determined by the formula in Eq. (1):

$$q_{vf}(x,y,z) = \frac{6\sqrt{3}f_f Q}{ac_b\pi\sqrt{\pi}} e^{-3\frac{x^2}{a^2}} \cdot e^{-3\frac{y^2}{c^2}} \cdot e^{-3\frac{z^2}{b_f^2}} \tag{1}$$

Table 1. Heat source dimension in FEM simulation

Heat source direction	Value (mm)
Width	4.0
Depth	4.0
Rear length	3.5
Front length	3.5

The heat flux power density in the rear section (Q_{vr}) can be calculated using Eq. (2):

$$q_{vr}(x,y,z) = \frac{6\sqrt{3}f_f Q}{ac_b\pi\sqrt{\pi}} e^{-3\frac{x^2}{a^2}} \cdot e^{-3\frac{y^2}{c^2}} \cdot e^{-3\frac{z^2}{b_f^2}} \tag{2}$$

In this context, f_f and f_r represent the fractional factors of heat deposition in the front and rear quadrants, respectively, with their sum equaling 2. The flux distribution in the double ellipsoid model is defined in four directions: width (a), depth (C), rear length (b_r), and front length (b_f). The values for each direction are provided in Table 1.

2. Virtual Manufacturing Using Nonlinear 3D-FEM Systems: Material Model, Process Parameters and Geometry

The integration of nonlinear 3D-FEM systems into virtual manufacturing frameworks offers a comprehensive approach to simulate real-world welding scenarios. This section presents the essential components required for accurate modeling, including material characteristics, process parameters and geometric configurations. These elements are crucial in ensuring that the simulation mirrors the actual physical behavior observed during laser welding processes.

2.1 Material Modelling

The simulation utilizes S235 low-carbon steel for both the welding and filler materials, reflecting the actual material employed in the welding process. The thermomechanical characteristics of S235 are illustrated in Figure 2, while the corresponding flow curve—based on an isotropic nonlinear hardening model—is also depicted. The parameters used in the simulation are summarized in Table 2 and are subsequently implemented during experimental validation using both FEM software platforms. Electrical current (I) and voltage (V) are factored into the power calculation and the welding travel speed (v) is selected based on the optimal speed for a one-pass T-joint configuration.

Figure 4 displays the geometrical setup, consisting of a base plate measuring 120 × 150 mm and a stiffener plate of 60 × 150 mm, both with a thickness of 4 mm to accommodate a double-sided weld. The model is meshed using a single-pass welding bead for this simulation.

This contemporary simulation methodology integrates thermal, mechanical and metallurgical phenomena into a unified numerical model, representing a significant advancement in engineering practices by replicating real-world manufacturing conditions. The inclusion of multiple physical domains enables a more in-depth and accurate analysis of welding behavior, capturing the complex interactions that occur concurrently. This comprehensive perspective enhances the ability to anticipate challenges such as residual stress, deformation and material deterioration, which are often difficult to evaluate using conventional approaches. Moreover, the simulation facilitates the optimization of welding variables, including heat input and cooling rates, to achieve target material properties. By incorporating real-time data from different stages of the process, the simulation also minimizes reliance on trial-and-error procedures, thereby reducing development time and associated costs.

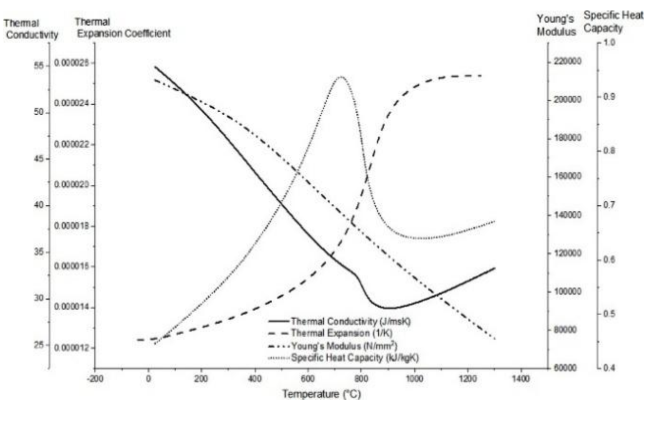

Figure 2. Temperature-dependent thermo-physical properties of S235

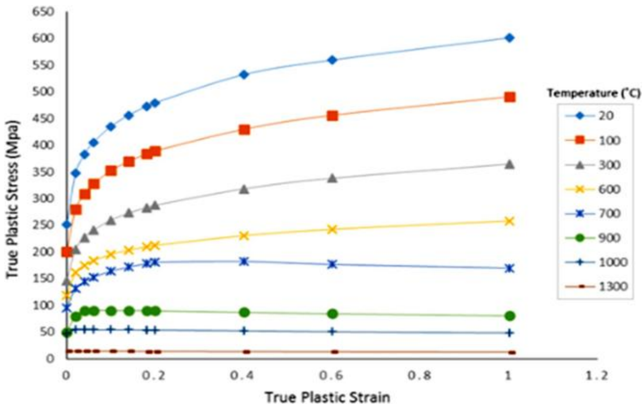

Figure 3: Flow curves of S235 steel at a strain rate of 10^{-3} s

Within the T-joint welding simulation, the material properties are customized using ANSYS Workbench. The process begins by accessing the “Engineering Data” section and selecting the “Edit” function, enabling users to modify material attributes according to the simulation’s requirements, as illustrated in the corresponding figure. This step is critical to ensure that the material definitions align accurately with the thermal and mechanical conditions expected during welding. Once these adjustments are made, the material becomes ready for application in the subsequent stages of the simulation.

To achieve realistic and reliable results, it is essential to input accurate values for key properties such as thermal conductivity, specific heat capacity and yield strength. These parameters play a vital role in determining heat transfer and stress distribution within the weld model. Additionally, the simulation setup should be calibrated to accommodate potential variations in material behavior under different temperature and loading conditions. Following the material definition, a well-structured mesh must be generated to precisely represent the weld zone. Proper meshing is fundamental to capture the complex interactions occurring during the welding process. Before proceeding with the full simulation, a preliminary run is recommended to evaluate the material’s performance under initial conditions. Any inconsistencies identified should prompt a reassessment of either the material properties or the meshing configuration to ensure simulation fidelity.

Table of Properties Row 16: Isotropic Thermal Conductivity

	A	B
1	Temperature (C)	Thermal Conductivity (W m^-1 K^-1)
2	25	54.938
3	200	50.625
4	400	43.578
5	600	36.776
6	700	34.154
7	750	33.117
8	800	32.276
9	850	27.711
10	1300	33.261
*		

Figure 4. Isotropic thermal conductivity set up using engineering data in Ansys

Table of Properties Row 19: Specific Heat Constant Pressure, C_p

	A	B
1	Temperature (C)	Specific Heat (J g^-1 K^-1)
2	25	0.44599
3	200	0.51679
4	400	0.61738
5	600	0.78967
6	700	0.94972
7	750	0.9355
8	800	0.85289
9	850	0.60113
10	1300	0.67086
*		

Figure 5. Spesific heat constant pressure set up using engineering data in Ansys

Table of Properties Row 5: Isotropic Secant Coefficient of Thermal Expansion

	A	B
1	Temperature (C)	Coefficient of Thermal Expansion (K^-1)
2	0	1.24E-05
3	50	1.26E-05
4	800	1.53E-05
5	850	2.53E-05
6	1250	2.54E-05
7	1466.9	2.54E-05
8	1517.2	0
*		

Figure 6. Isotropic secant coefficient of thermal expansion set up using engineering data in Ansys

Table of Properties Row 9: Isotropic Elasticity

	A	B	C	D	E
1	Temperature (C)	Young's Modulus (MPa)	Poisson's Ratio	Bulk Modulus (Pa)	Shear Modulus (Pa)
2	25	2.1063E+05	0.3	1.7552E+11	8.101E+10
3	300	1.9341E+05	0.3	1.6118E+11	7.4389E+10
4	500	1.7141E+05	0.3	1.4284E+11	6.5928E+10
5	900	1.1676E+05	0.3	9.7303E+10	4.4909E+10
6	1300	75692	0.3	6.3077E+10	2.9112E+10
*					

Figure 7. Isotropic elasticity set up using engineering data in Ansys

2.2 Process Parameters

This section presents the fundamental process parameters employed in simulating welding-induced distortions in T-joints. Parameters such as electrical current, voltage, welding travel speed, and heat transfer coefficients have been carefully chosen to align with the characteristics of the welding technique and materials involved. These parameter values are critical to replicating real-world welding conditions within the simulation environment, thereby enabling precise prediction of thermal and mechanical responses throughout the welding process.

Table 2. Welding parameters used in both FEM software

Welding Parameter	Value
Current (A)	200
Voltage (V)	20
Travel Speed, v (mm/s)	67
Latent Heat (J/kg) or (mm²/s²)	256400 or 2564e+11
Liquidus Temperature (°C)	13000
Solidus Temperature (°C)	12950
Contact Heat Transfer Coefficient (W/m²K) or (N/mm²K)	1000 or 1
Convective Heat Transfer Coefficient (W/m²K) or (N/mm²K)	20 or 0.02
Emissivity Coefficient (-)	0.6

The impact of each process parameter on both distortion and the structural integrity of the welded joint is thoroughly evaluated, offering in-depth insights into the interdependence between these variables and the resulting weld quality. This assessment enables the identification of key factors that most significantly contribute to common welding defects such as warping, cracking and incomplete fusion. Parameters like heat input, welding speed and material characteristics are instrumental in shaping the final weld outcome. Through simulation-based adjustments of these parameters, engineers can investigate multiple welding scenarios and fine-tune the process to meet targeted weld performance criteria. Moreover, the simulation facilitates an understanding of how variations in one parameter may influence others, highlighting the need for a carefully managed balance among all variables. The predictive capability of the simulation to foresee potential distortions and defects prior to actual welding is highly beneficial in minimizing rework and material waste. Additionally, recognizing how these parameters affect the material's microstructure enhances control over the mechanical properties of the finished weld. Such comprehensive simulation-driven analysis is indispensable for achieving consistent, high-quality welds in complex manufacturing environments.

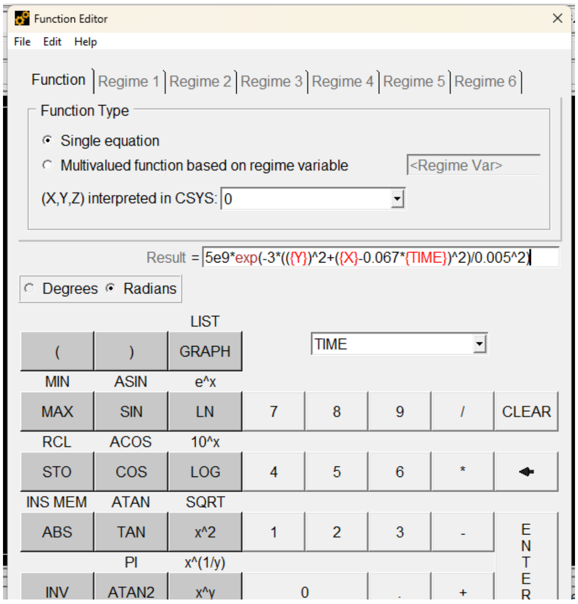

Figure 8. Process parameters set up using Mechanical APDL

Ansys Mechanical APDL conducts finite element method (FEM) simulations utilizing well-established principles, providing a unique range of features specifically designed for its script-driven interface.

Ansys Mechanical APDL supports an extensive simulation workflow, functioning as a versatile FEM platform capable of addressing a broad spectrum of engineering challenges, including welding analyses. Figure 9 presents a schematic depiction of the finite element model constructed using Ansys 2024 R2. The CAD geometry was developed in Ansys SpaceClaim, incorporating weld bead representations along the T-joint to simulate the welding path accurately. Within APDL, users are granted comprehensive control over meshing techniques, boundary condition definitions and load step configurations through a scripting-based approach, enabling highly tailored simulations. However, this level of flexibility necessitates a strong grasp of FEM fundamentals and proficiency in the APDL scripting language.

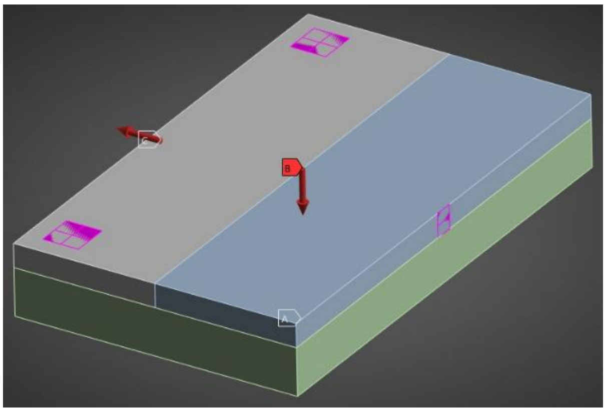

Figure 9. FE model of 3D solid welded T-joint using Ansys 2024 R2

3. Experimental Setup and Procedures of Welded Butt Joint

A comprehensive set of experimental welding procedures was conducted to validate the FEM simulation outcomes using a butt joint configuration. The welding setup featured a TruDisk 4002 laser source with a power capacity of 4000 W, integrated with a TRUMPF robotic arm for precise manipulation. The laser head was equipped with a shielding gas nozzle that supplied argon gas at a flow rate of 21 L/min, ensuring adequate protection of the weld zone throughout the process. The test specimens comprised dissimilar materials and potential welding defects were minimized through proper surface preparation and cleaning prior to welding. An illustration of the robotic welding system is provided in Figure 10. The experimental procedure was carefully aligned with the simulation parameters to ensure consistency and comparability of results. Data collected during the welding trials included thermal profiles, distortion measurements, and visual inspection of the weld seam. These data sets served as critical benchmarks for evaluating the accuracy of the FEM model. Furthermore, high-speed imaging and post-weld microstructural analysis were employed to gain deeper insights into the weld dynamics.

Figure 10. TRUMPF Robotic Arm

Table 3. Chemical composition of material S235

Elements	S235 (Data Sheet)	Low Carbon Steel (Experiment)
C	0.15	0.186
Mn	1.1	0.146
Si	-	0.011
S	0.027	0.0011
P	0.02	0.001

Table 3 presents the chemical composition of S235 based on the material data sheet and the experimental results acquired with an Arc Spark Emission Spectrometer.

A high-precision Zeiss Calypso Coordinate Measuring Machine (CMM) was employed to assess distortion at various points along the edges of the plate. Measurements were taken at identical locations on the specimens both prior to and following the welding process to obtain the final data. Three specific points on the plate were chosen for evaluating angular distortion.

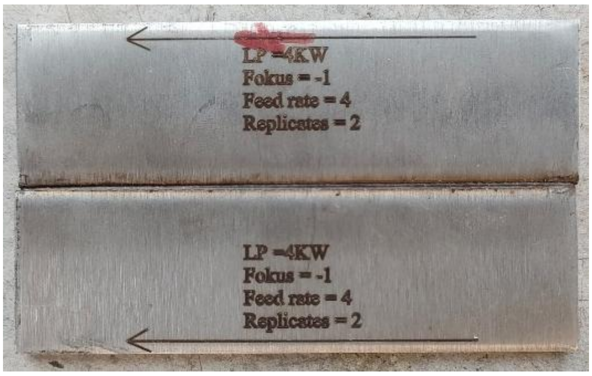

Figure 11. Top view of distortion result in butt joint experiment

Figure 12. Bottom view of distortion result in butt joint

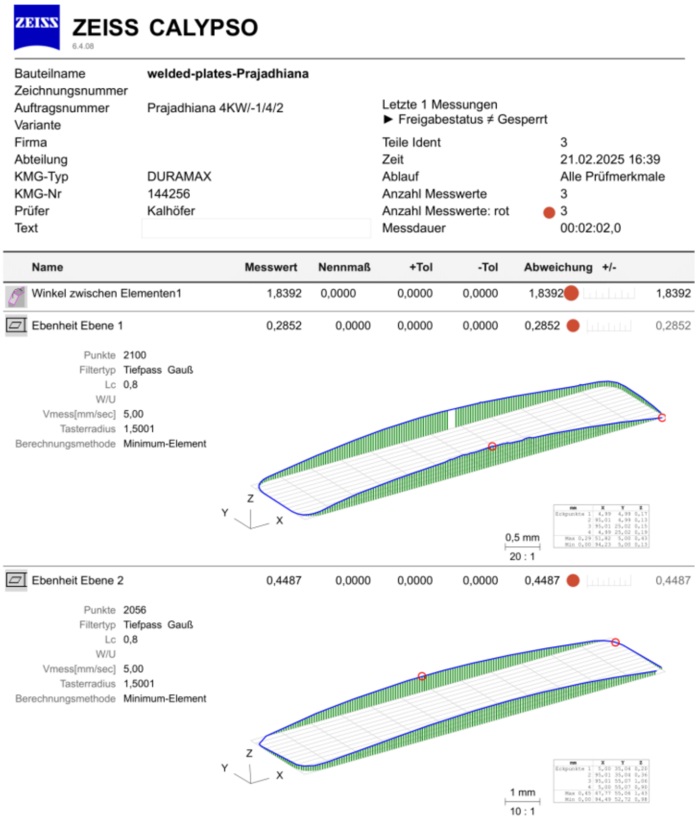

Figure 13. Maximum distortion result with Zeiss Calypso coordinate measuring machine

4. Result and Discussion

Figures 12 and 13 present the angular distortion results based on displacements obtained from both the finite element method (FEM) simulation of the solid model and the experimental procedure. The maximum displacement points were designated as tracking points to evaluate distortion in both approaches. To ensure a valid comparison, the points selected in the FEM simulation matched those measured using the CMM in the experimental process. These tracking points were deliberately positioned in regions anticipated to exhibit significant distortion, allowing for the identification of critical deviations in the welded joint. The comparison between FEM and experimental data serves as a comprehensive validation of the simulation model, confirming its ability to replicate the material's actual behavior under welding conditions. Additionally, this comparison facilitates the identification of inconsistencies or limitations within the simulation, which can subsequently be addressed to enhance its accuracy. The findings from both methods offer valuable insights into the welding process, particularly regarding the extent of angular distortion and its implications for joint integrity. This analysis enables the refinement of welding parameters, such as heat input and cooling rates, to effectively reduce distortion.

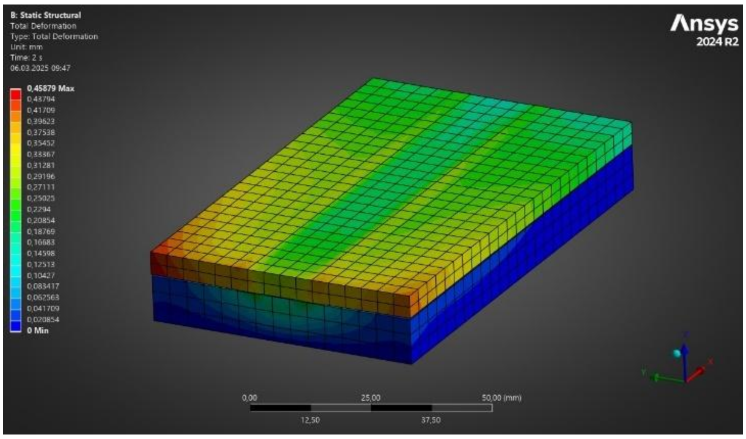

Figure 14. Total deformation result in butt joint using

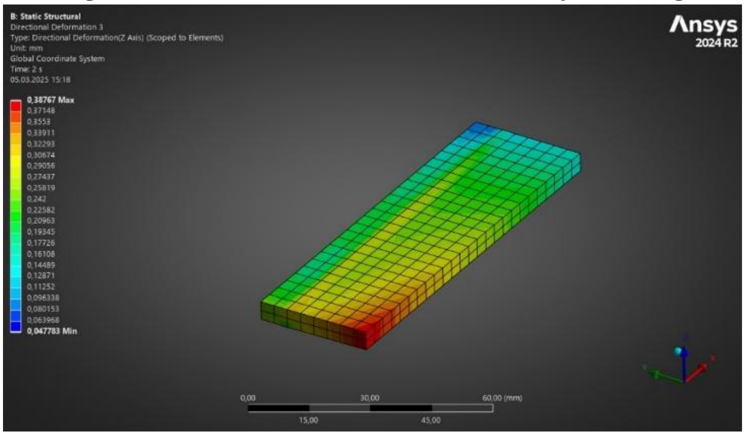

Figure 15. First side of angular distortion result in Butt joint using APDL

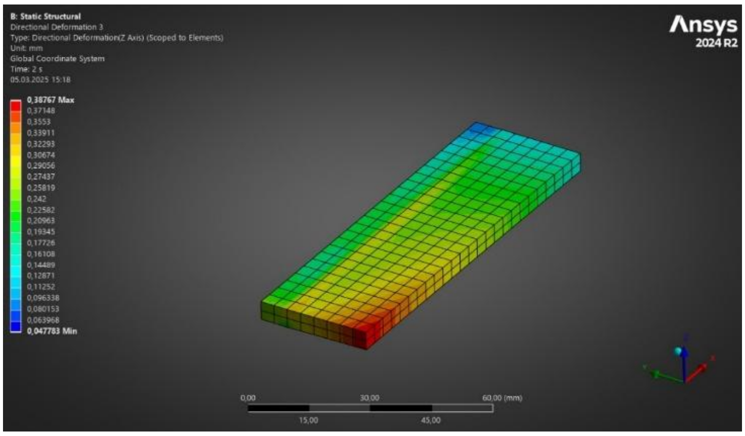

Figure 16. Second side of angular distortion result in Butt joint using APDL

Table 4. Pre-processing time ruquired for modfelling to execution

Non-linear VM Tool	Pre-processing time (s)
Ansys APDL	353

Table 5. Computational time required for simulation in butt joint simulation

FEM System	Computational time (s)
Ansys APDL	1097

Table 6. Simulation and experimental result comparison in butt joint

Position	Maximum angular distortion (mm)		Relative error (%)
	Experiment	Ansys APDL	Ansys APDL
1^{st} side	0.29	0.38	31
2^{nd} side	0.44	0.40	9

In the final analysis of the butt joint, a comparison was conducted between the numerical simulation results and the experimental data. For the second side, the findings indicate minimal discrepancy, with the numerical simulation yielding a distortion of 0.40 mm and the experimental result showing 0.44 mm, corresponding to a relative error of 9%. Conversely, the first side also demonstrates acceptable accuracy, as the numerical and experimental results, 0.38 mm and 0.29 mm, respectively, result in a relative error of 31%. Despite this higher percentage, the absolute difference remains small (less than 0.5 mm), and thus, the results are deemed sufficiently accurate. The variation observed on the first side may be attributed to minor inconsistencies in the experimental setup, such as subtle deviations in welding parameters or material characteristics. Additionally, this difference may stem from inherent limitations within the simulation model, which may not fully capture all real-world influences affecting the welding process. Nonetheless, the overall consistency between the simulation and experimental outcomes affirms the reliability of the numerical model. The notably low error observed on the second side further substantiates the validity of the simulation approach. Future studies may aim to enhance both simulation accuracy and experimental precision by incorporating more comprehensive models that account for factors such as thermal cycles, residual stresses and material behavior.

5. Conclusion

A study on the distortions of welded butt joints using Laser Welding has been conducted through FEM-based Virtual Manufacturing. The research includes both numerical and experimental analyses, with the final results compared. The numerical analysis was performed using Simufact Welding and Ansys APDL software, employing 3D solid elements. The key conclusions of the research are as follows:

1. The FEM-based Virtual Manufacturing of the butt joint model was successfully carried out, with a clear and simplified simulation procedure.
2. The Virtual Manufacturing modeling and simulation using Ansys APDL showed good agreement with the distortion tendencies observed in the experimental results.
3. Ansys APDL provided stable results, with a lower average error percentage of 20%, showing minimal difference, even less than 0.5 mm.
4. Ansys APDL demonstrated fast Pre-Processing and computational times, with 353 seconds for Pre-Processing and 1097 seconds for Post-Processing.
5. Due to the simplified procedure, complex factors such as the heat source and thermal calibration could be neglected.
6. Ansys APDL offers a straightforward procedure and is easier to use compared to general-purpose Virtual Manufacturing tools.
7. Variations in non-homogeneous materials, geometry, pre-conditions of the welding process, and fluctuating experimental parameters may explain the differences between the simulation and experimental results.

From a knowledge perspective, valuable insights obtained through simulation can be used as a planning tool during the design phase or prior to the actual welding process. This research could contribute to the further development of FEM-based Virtual Manufacturing applications, such as for other joint geometries and materials. By incorporating more complex material models and heat transfer dynamics, simulations can more accurately predict welding behavior and minimize potential defects. Moreover, these insights can be utilized to enhance quality control measures, reducing the likelihood of post-weld issues and improving overall manufacturing efficiency. As computational power continues to grow, the potential for real-time simulation and adaptive welding strategies will increase.

ACKNOWLEDGEMENT

The authors wish to extend their profound gratitude to God Almighty for His continuous guidance and blessings throughout the course of this research. The successful completion of this study would not have been possible without His divine intervention.

Sincere appreciation is conveyed to the advisors, Prof. Dr. Eng. Himsar Ambarita, ST., MT., Prof. Ts. Ir. Dr. Ing. Yupiter Harangan Prasada Manurung, and Prof. Dr. Ing. Miranda Fateri, for their invaluable technical expertise and personal mentorship throughout the research. Their insight, commitment, and unwavering support have been instrumental to the success of this work.

The authors also acknowledge the constructive input provided by the first and second reviewers, whose feedback greatly enhanced the quality of this research. Gratitude is extended to Dr. Ir. M. Sabri, M.T., IPM., Asean Eng., and Mr. Suprianto ST., MT., Ph.D., for their leadership within the Department of Mechanical Engineering at FT-USU Medan, as well as to all faculty and staff members for their continued support and encouragement.

This research was generously supported by the German Academic Exchange Service (DAAD) under the project "Additive Manufacturing and Welding: Simulation, Process, and Application for Earth and Space," conducted at Aalen University, Germany.

The authors also express their appreciation to their colleagues, Dr. Keval Priapratama Prajadhiana and Muhammad Zulhilmi Bin Mohd Izhar, for their collaboration and camaraderie during the research period in Germany.

Lastly, heartfelt thanks are extended to the authors' families, friends, and peers for their unwavering support and encouragement throughout this journey.

This work is dedicated to the advancement of knowledge and the continuous development of the engineering discipline, and to all individuals who contributed to its realization.

References

[1] Wang, Q., "Virtual Manufacturing and Systems," WIT Transactions on State-of-the-Art in Science and Engineering, Vol. 16, 2005.

[2] Bharath, V. and Rajashekar, P., "Virtual Manufacturing: A Review," International Journal of Engineering Research & Technology, Vol. 3, No. 17, pp. 355-364, 2015.

[3] Shukla, C., Vazquez, M., and Chen, F. F., "Virtual Manufacturing: an Overview," Computers & Industrial Engineering, Vol. 31, Nos. 1-2, pp. 79-82, 1996.

[4] Cao, X., and Nolting, A., "Autogenous Fiber Laser Welding of 70/30 Cu-Ni Alloy Plates," *Materials and Design*, Vol. 181, Article 108075, pp. 1–10, 2019.

[5] Yazdian, N., "Hybrid Laser/arc Welding of Difficult-to-Weld Thick Steel Plates in Different Joint Configurations: Issues and Resolutions," *Ph.D. Dissertation*, Department of Mechanical Engineering, Southern Methodist University, Dallas, TX, 2019.

[6] Zeghida, C., and Guedri, A., "Effects of Welding Sequences on Residual Stresses in a Butt Joint of Austenitic Piping," *Acta Mechanica Slovaca*, Vol. 27, No. 3, pp. 28–40, 2023.

[7] Vetriselvan, R., Devakumaran, K., Sathiya, P., and Ravichandran, G., "Transient Out-of-Plane Distortion of Multi-Pass Fillet Welded Tube to Pipe T-Joints," Defence Technology, Vol. 13, No. 2, pp. 77-85, 2017.

[8] Okano, S. and Mochizuki, M., "Transient Distortion Behavior during Tig Welding of Thin Steel Plate," Journal of Materials Processing Technology, Vol. 241, pp. 103-111, 2017.

[9] Bajpei, T., Chelladurai, H., and Ansari, M. Z., "Experimental Investigation and Numerical Analyses of Residual Stresses and Distortions in GMA Welding of Thin Dissimilar AA5052- AA6061 Plates," Journal of Manufacturing Processes, Vol. 25,pp. 340-350, 2017.

[10] Robert, W. and Messler, J., "Principle of Welding: Processes, Physics, Chemistry, and Metallurgy," John Wiley & Sons, 2008.

[11] Kim, M., Kang, M., and Chung, H., "Simplified Welding Distortion Analysis for Fillet Welding Using Composite Shell Elements," International Journal of Naval Architecture and Ocean Engineering, Vol. 7, No. 3, pp. 452-465, 2015.

[12] Sun, J., Liu, X., Tong, Y., and Deng, D., "A Comparative Study on Welding Temperature Fields, Residual Stress Distributions and Deformations Induced by Laser Beam Welding and CO_2 Gas Arc Welding," Materials & Design, Vol. 63, pp. 519-530, 2014.

[13] Wang, C., Kim, Y. R., and Kim, J. W., "Numerical Modelling of Welding Distortion Redistribution due to the Change of Self- Constraint in a T-Joint Welded Structure," Journal of Mechanical Science and Technology, Vol. 30, No. 6, pp. 2683-2690, 2016.

[14] Wang, J., Yuan, H., Ma, N., and Murakawa, H., "Recent Research on Welding Distortion Prediction in Thin Plate Fabrication by Means of Elastic FE Computation," Marine Structures, Vol. 47, pp. 42-59, 2016.

[15] Deng, D., Liang, W., and Murakawa, H., "Determination of Welding Deformation in Fillet-Welded Joint by Means of Numerical Simulation and Comparison with Experimental Measurements," Journal of Materials Processing Technology, Vol. 183, Nos. 2-3, pp. 219-225, 2007.

[16] Barsoum, Z. and Lundback, A., "Simplified FE Welding Simulation of Fillet Welds-3D Effects on the Formation Residual Stresses," Engineering Failure Analysis, Vol. 16, No. 7, pp. 2281-2289, 2009.

[17] ISO 14341, "Welding Consumables - Wire Electrodes and Weld Deposits for Gas Shielded Metal Arc Welding of Non Alloy and Fine Grain Steels - Classification," 2010.

[18] Perić, M., Garašić, I., Gubeljak, N., Tonković, Z., Nižetić, S., and Osman, K., "Numerical Simulation and Experimental Measurement of Residual Stresses in a Thick-Walled Buried-Arc Welded Pipe Structure," *Metals*, Vol. 12, No. 7, pp. 1–14, 2022.

[19] Peric, M., Tonkovic, Z., Rodic, A., Surjak, M., Garasic, I., et al., "Numerical Analysis and Experimental Investigation of Welding Residual Stresses and Distortions in a T-Joint Fillet Weld," Materials & Design, Vol. 53, pp. 1052-1063, 2014.

[20] Chujutalli, J.H., Lourenço, M.I., Estefen, S.F., "Experimental-based methodology for the double ellipsoidal heat source parameters in welding simulations," Marine Systems & Ocean Technology, Vol. 15, pp. 110–123, 2020.